Materials Research.
DOI: http://dx.doi.org/10.1590/1980-5373-MR-2017-0324

Mechanical Characterization of Basalt and Glass Fiber Epoxy Composite Tube

Mauro Henrique Lapena[a]*, Gerson Marinucci[b]

[a]Divisão de Materiais, Instituto de Aeronáutica e Espaço - IAE, Departamento de Ciência e Tecnologia Aeroespacial - DCTA, Praça Marechal Eduardo Gomes, 50, Vila das Acácias, 12228-900, São José dos Campos, SP, Brazil
[b]Instituto de Pesquisas Energéticas Nucleares, IPEN - CNEN/SP, Av. Prof. Lineu Prestes, 2242, 05508-900, São Paulo, SP, Brazil

Received: March 28, 2017; Revised: August 07, 2017; Accepted: September 18, 2017

The application of basalt fibers are possible in many areas thanks to its multiple and good properties. It exhibits excellent resistance to alkalis, similar to glass fiber, at a much lower cost than carbon and aramid fibers. In the present paper, a comparative study on mechanical properties of basalt and E-glass fiber composites was performed. Results of apparent hoop tensile strength test of ring specimens cut from tubes and the interlaminar shear stress (ILSS) test are presented. Tensile tests using split disk method provide reasonably accurate properties with regard to the apparent hoop tensile strength of polymer reinforced composites. Comparison between the two tubes showed higher basalt fiber composite performance on apparent hoop tensile strength (45% higher) and on the interfacial property interlaminar shear stress (ILSS) (11% higher). New data obtained in this work on basalt fiber composite tubes confirm the literature for basalt fiber composite with other geometries, where it overcomes mechanical properties of the widely used glass fiber composites.

Keywords: *basalt fiber, glass fiber, polymer matrix, filament wound tube, split disk*

1. Introduction

Basalt is volcanic mineral, dark or black. Its rocks are heavy, tenacious and resilient. Basalt density is about 5% higher than the glass. It's the most abundant crustal rock and the seabed is predominantly composed of basalt. The chemical composition of the basalt is variable according to the mineral deposit. The weight percentage of the constituent oxides: SiO_2, 48,8-51; Al_2O_3, 14-15,6; CaO, ≈10; MgO, 6,2-16; FeO + Fe_2O_3, 7,3-13,3; TiO_2, 0,9-1,6; MnO, 0,1-0,16; Na_2O + K_2O, 1,9-2,2[1].

Current technology for producing basalt fibers (BF) is very similar to that used in E-glass fiber (GF) production[2]. This fact, coupled with the high availability of raw material around the world, justifies the low price of BF compared to GF. The main difference between the BF and GF is the raw material used. GF are produced from various components, while BF is made with the fusion of basalt rock without other additives. BF are environmentally friendly, what makes its use very attractive; unlike GF, BF does not require additives in their production. The replacement of GF by BF can reduce the risk of environmental pollution with highly toxic metals and oxides, which are generated in the production of GF[3,7]. Moreover, BF is an alternative to asbestos fibers, banned for being carcinogenics.

Basalt fibers are competitive with glass fibers, being a good alternative to them as reinforcing material in composites used in several fields such as marine, automotive, sporting, civil, etc[4]. It exhibits excellent resistance to alkalis, similar to GF, at a much lower cost than carbon and aramid fibers. Its thermal properties allows substitution of high temperature resistant fibers (carbon fibers) and its working temperature is higher than GF - the onset temperature of decomposition in the presence of air is 205 °C, and 164 °C in the case of GF[5,6].

The dynamic behavior of epoxy/BF composite (including damping ratio) is similar to epoxy/GF composite[7]. Polymer/BF reinforced composite presented water absorption of 0.33% (in weight), against 0.38% for polymer/GF and 0.55% for polymer/carbon fiber[1]. Its high water resistance also explains the wide application in the marine industry, as in production of boat hulls[8]. For their good electrical insulation properties (10 times greater than glass)[3,9], BF are used in printed circuit boards, extra-thin insulation for electrical cables and underground pipelines.

Regarding the mechanical properties, BF overcomes GF 15% in elastic modulus and 11% in tensile strength[8,10]. These various similarities motivated comparisons between their polymer reinforced composites which found promising potential use for BF in fields where GF is already largely applied[11,12,13].

Experimentally measuring the load carrying capacity of a vessel can be expensive and impractical given the different design configurations possible by changing the layup[14]. So, one alternative normally used by the laboratories and industries is perform tests by the split disk method. Many

*e-mail: maurolapena@gmail.com

research studies have been found in the literature concerned with this methodology[15,16], being to a lesser extent referring epoxy/basalt fiber composites. Study regarding mechanical properties of tubular geometry basalt composite was made[13], where tensile properties of glass, carbon and basalt fiber reinforced/epoxy composite cylinders made by filament winding were reported, using a proprietary test method; BF composite presented higher tensile strength and modulus than GF composite. Filament wound GF and BF composite tubes were submitted to internal pressurization for degradation assessment of flame-sprayed aluminum deposition process. The coated tubes exhibited reduced burst strengths.

Parametric studies were conducted[15] on filament wound composite tubes reinforced with glass fiber, with the aim to determine minimum length that can represent an infinite tube in hydrostatic testing, to find the optimum wind angle of composite tubes subjected to internal pressure under different end conditions and to study the influence of diameter and thickness on the failure pressure during tube burst tests. Split disk tests were done with specimens cut from a composite tube $[\pm 55°]_4$ to compare the resulting apparent hoop fracture stress with the hoop stresses obtained from the models, and the calculated hoop stresses reached 89% for closed-end, 85% for restrained-end and 62% for open-end condition.

Processing parameters were investigated[16] of filament wound composite tubes with glass and carbon fiber using different winding angles. Results of split disk test were obtained with low standard deviations. Fiber fracture and fiber matrix debonding was observed to be the dominant failure mechanisms for specimens having 90° winding angle. For specimens having ±25° winding angle, fiber breakage was very limited and the specimens failed with the rupture of the matrix phase.

This paper compares and discusses the mechanical properties of BF and GF composite tubes obtained by filament winding. The aim is to verify the suitability of using BF as an option to replace GF and enlarge the available experimental results with new data. Interfacial property ILSS was measured and apparent hoop tensile strength test was carried out using split disk (ring segment) test, which results in hoop stresses similarly if specimens were under internal pressure.

2. Materials and Method

2.1. Materials

The BF was supplied by Kammeny Vek (Russia) in continuous filament with a linear density of 1200 tex, made from fibers of 13 μm diameter, with silane agent sizing compatible with epoxy and phenolic resins. E-glass fiber was supplied by CPIC (Brazil) in continuous filament with a linear density of 2000 tex, with silane agent and sizing compatible with epoxy and amine resins. The matrix was resin epoxy-bisphenol A diglycidyl ether, with initiator methyl tetrahydrophthalic hardener and curing promoter benzyl-dimethylamylamine.

2.2. Methods

Configuration of deposited layers was defined considering works with similar production or test methods[18,25], tube strength in longitudinal and transverse direction and number of layers. One function of layers wound at 0º angle is to provide strength and rigidity over the circumferential direction, the same direction the load is applied in split disk test.

BF and GF reinforced epoxy laminates tubes with open-ended cylinder geometry were manufactured by filament winding. The winding parameters such as filament tension, die angular speed and carriage longitudinal speed were controlled by a CNC. The coordinate movement of these two axes established the fiber deposition angles over the mandrel.

Three filament winding tubes were manufactured with BF and another three with GF reinforcement, each one six plies following the stacking sequence $[90º_2/-30º/+30º/90º_2]_T$.

The composite tube was made by superposition winding method, as shown in Figure 1. In this method, the helical layers (-30º and +30º) are independently positioned. First, as shown in Figure 1(a), the entire layer at -30º was wound over the preceding hoop layer, and afterwards the +30º layer, as shown in Figure 1(b). Differently from the interweaving winding method, where the filament of -30º is crossed over the filament of +30º in each cycle of forward-backward travel of the car in the filament winding machine. In the superposition winding method the domes are composed of pins, radially positioned in a metallic disc, instead of those used in interweaving winding method, with geodesic shape.

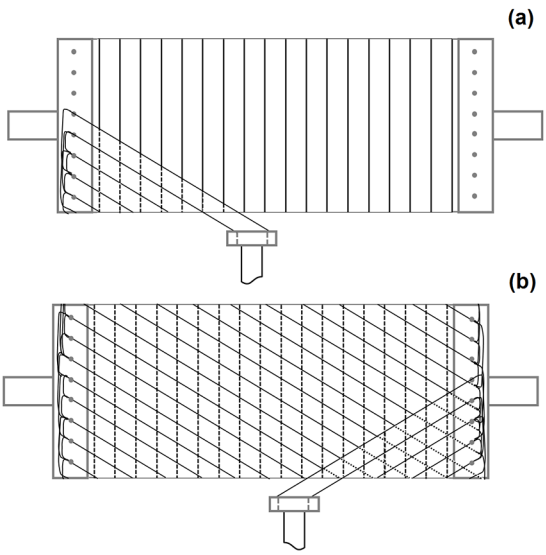

Figure 1. Schematic of superposition winding method for helical layers. Filament winding process at (a) -30º layer and at (b) +30º layer.

After filament winding process, the mold was placed to oven for a curing cycle of 8h, reaching a maximum temperature of 150°C.

Ring specimens of 10 mm wide were cut from opposite ends of each tube, using a diamond saw (6 total specimens of each BF and GF composite). Apparent hoop tensile strength split disk test was carried out according to ASTM D2290 - Procedure A[19] specifications, although with alteration in specimens' geometry - according to the standard, the specimens shall have minimum overall width of 22.86 mm and at least one reduced section, with minimum width of 13.97 mm. An apparent tensile strength rather than a true tensile strength is obtained in this test because of a bending moment imposed during test at the split between the split disk test fixture. The apparent hoop tensile strength was calculated using the following equation:

$$\sigma_a = \frac{P_b}{2A_m}$$

where σ_a is the ultimate tensile stress (MPa) of the specimen, P_b is the maximum load and A_m is the minimum cross-sectional area of the two measurements.

For ILSS tests, specimens were cut from rings of 10 mm length, with dimensions 10 x 20 mm. The shear strength was calculated using the equation given by:

$$ILSS = 0,75\frac{P_m}{bh}$$

where *ILSS* is the interlaminar shear strength (MPa), P_m is the first drop in measured load, b is the measured specimen width and h is the measured specimen thickness.

Differential scanning calorimetry (DSC-Perkin Elmer Pyris) was performed at nitrogen atmosphere, from 25 to 180 °C at heating rate of 20 °C.min $^{-1}$. Volume fraction was measured using matrix burn method at temperature of 565 °C in accordance with ASTM D3171 - 15 [20].

3. Results and Discussion

3.1. Physical characterization

The glass transition temperature (T_g) in thermosetting polymers is characterized by the region where is a slope change in the DSC analysis curve. Glass transition temperature (T_g) around 128ºC for both BF and GF composites was obtained by DSC analysis, as can be seen in Figure 2. The very close results of T_g for BF and GF composites evidences steady curing process at oven as well same degree of cure in both composites [21]. In matrix burn test method, it was obtained fiber volume fraction of 55% and void volume fraction of 3%, for both BF and GF composites.

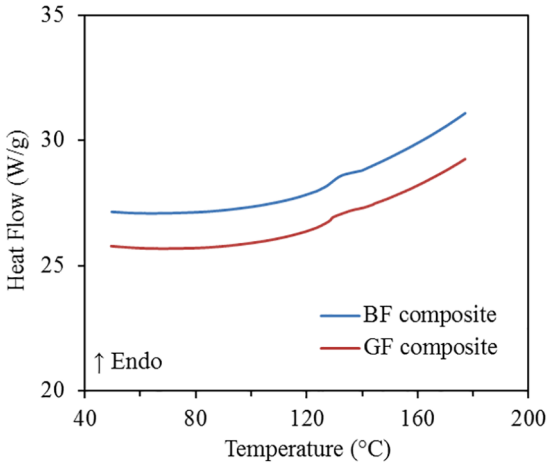

Figure 2. DSC curves for BF and GF composites.

3.2. ILSS test

Supports span in the interlaminar shear strength test apparatus was set in order to achieve a span-to-medium thickness ratio of 4. The mean thickness of the BF and GF composite specimens was 1.58 and 2.58 mm, respectively. From the simple beam theory for a three point bending for a rectangular specimen, the maximum interlaminar shear value is achieved at the thickness midplane. ILSS test is a three point bending test where the support span is minimized to maximize the shear tensions.

The morphology of fractured specimens has been examined to identify characteristic failure features, by means of optical microscopy. Figure 3(a) shows BF composite and Figure 3(b) shows GF composite specimens after ILSS test. Regions near the loading point of a BF and a GF composite specimen are shown in detail in Figures 3(b) and 3(d) respectively. Fiber rupture in the opposite side of loading point is characteristic of (i) tension failure mode. Crack located around thickness midplane indicates (ii) interlaminar shear failure mode. The imprint found in the loading point region is characteristic of (iii) inelastic deformation failure mode. These mentioned modes of failure are illustrated in ASTM D2344 - 13[22].

Typical load-displacement curves are shown in Figure 4. The initial non linear aspect of the curves is possibly a spurious region, referred to as "toe region", which can be caused by seating of the specimen[21]. At the remaining portion of the curve, the load increases linearly as the displacement increases, until the maximum value. The ILSS value was calculated using the maximum load, registered at first load drop off.

ILSS tests were performed[11] for BF and GF composites with plain-weave woven fiber fabrics and epoxy matrix following also ASTM D2344, and the results were 41 and 36 MPa, respectively. The value of 47.5 MPa was found[23] following the same standard in unidirectional GF composite. In the present work the experimental values found were 70.1

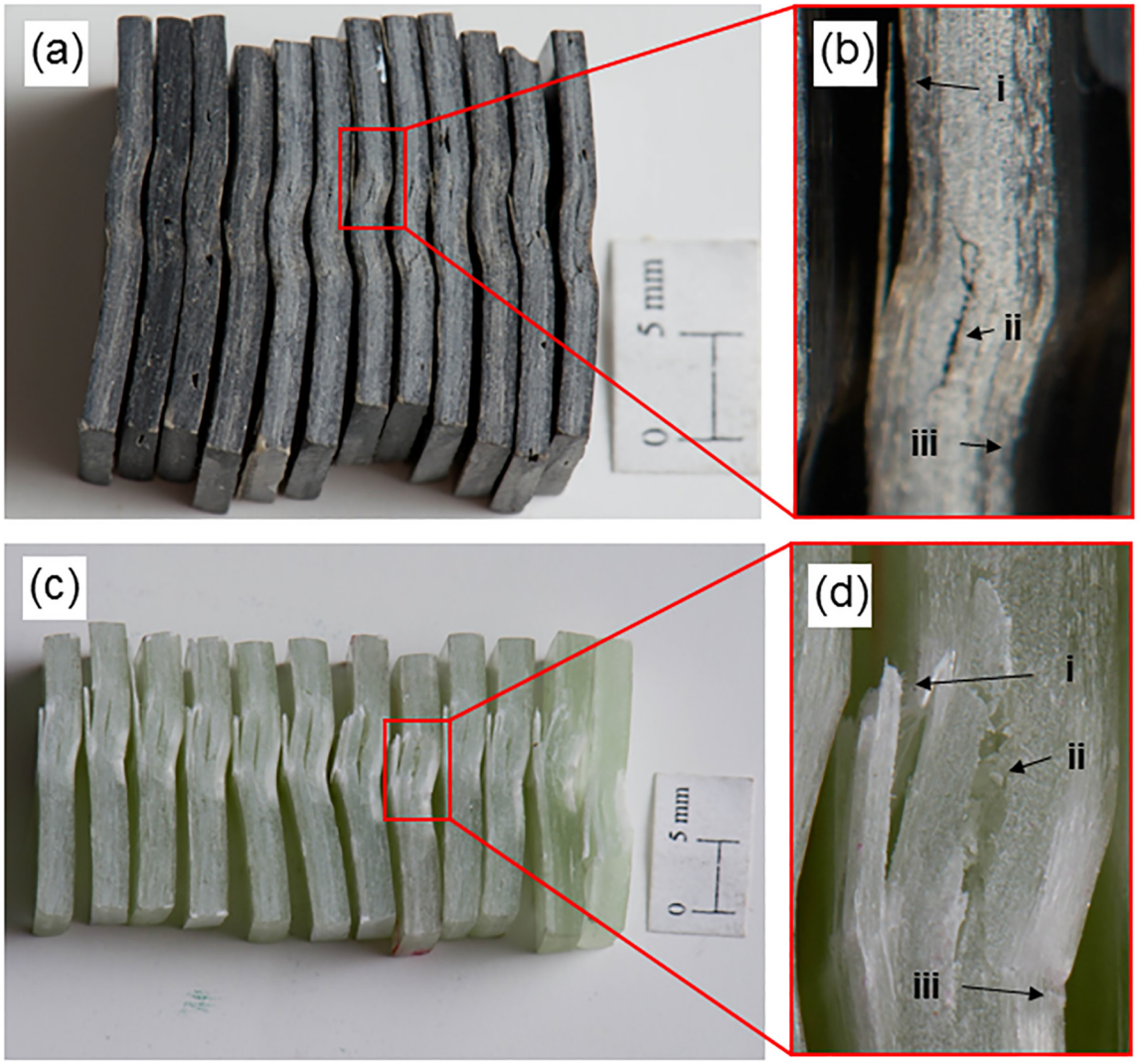

Figure 3. Aspect of (a) BF and (c) GF composite specimens after ILSS test. Identification of failure modes in (b) BF and (d) GF specimens; (i) tension failure, (ii) interlaminar shear, (iii) inelastic deformation.

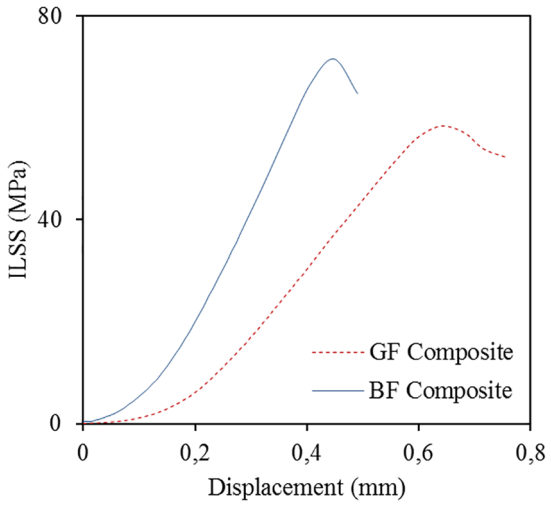

Figure 4. Typical load-displacement curves during ILSS test of BF and GF composite.

and 62.9 MPa respectively for BF and GF composites, higher values than the aforementioned. Comparison between found values is shown in Figure 5, and indicates good interfacial adhesion obtained in embedding BF and GF in the epoxy matrix. The higher value of ILSS for BF composite than GF composite indicates better interfacial adhesion between BF and the epoxy matrix than GF. Furthermore, probably the interface between the layers of -30° and +30° promotes greater interlaminar shear strength than interfaces between layers of plain-weave fabric and between unidirectional interface layers.

Regarding fiber/matrix interfacial adhesion, the relation between ILSS and IFSS (interfacial shear strength) was already reported[24]. Mechanical tests like IFSS were generally accepted to characterize the quality of adhesion. Fiber-bundle pull-out test (IFSS) was performed on carbon fiber/epoxy composite and ILSS was also conducted to indirectly reflect

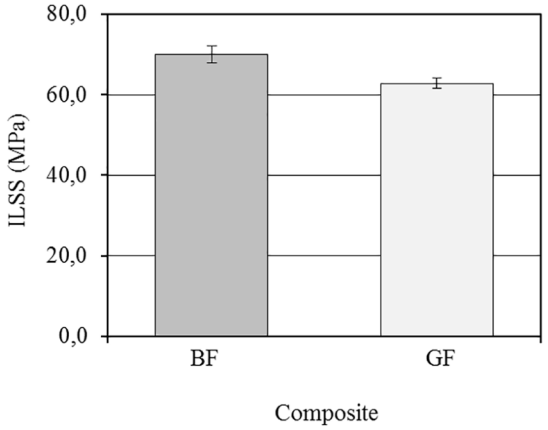

Figure 5. ILSS of BF and GF composites.

the reliability of the test. ILSS results presented a trend that coincides with IFSS. So, one can see that the higher ILSS for BF composites can indicate better fiber/matrix adhesion than GF composites, that represents a more efficient load transfer from matrix to reinforcements and consequently a better structural behavior.

3.3. Split disk test

Figure 6 shows typical load-displacement curves for BF and GF composites. It is found that the applied load increases linearly to the maximum value as the displacement increases. Failure occurs with brittle behavior, to the extent that there is a sharp drop in load.

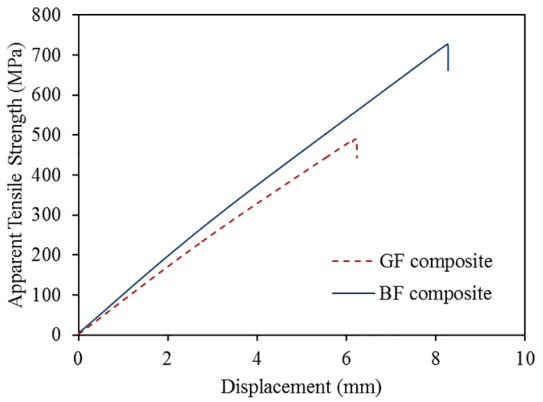

Figure 6. Split disk test tensile-displacement curves of BF and GF composites.

For BF composite specimen shown in Figure 7(a, b, c), from a failure analysis/fractography perspective, it is observed, on plies of 90° winding angles (internal and external plies), fiber-matrix debonding, intralaminar fracture and fiber fracture. In the -30° and +30° plies (internal to 90°) is observed intralaminar fractures along circumferential direction.

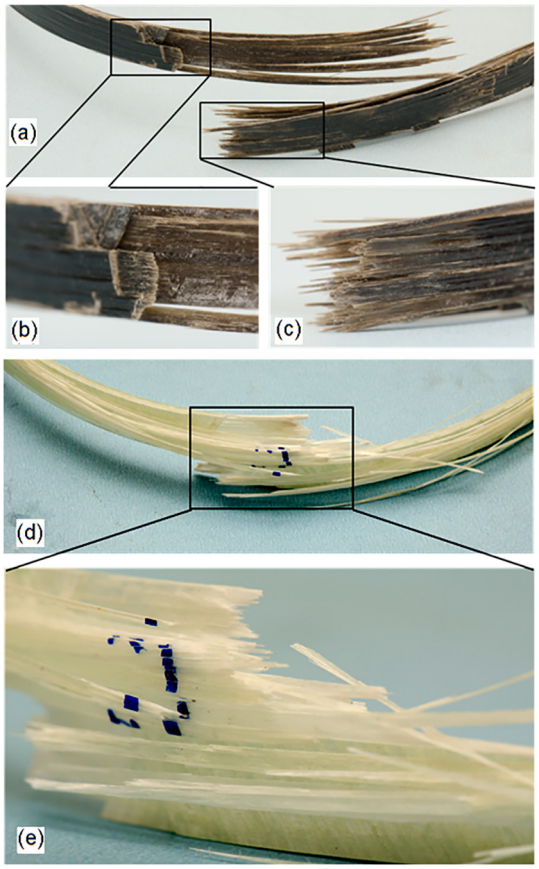

Figure 7. (a) BF and (d) GF ring segment specimen failure. Detail view of (b, c) BF and (e) GF specimens.

Delaminations (interlaminar fracture) are observed in the interface between plies -30°/ 90°, and in +30°/ 90°. For GF composite ring segment specimen, as seen in Figure 7(d, e), internal and external plies of 90° winding angle suffer fiber fracture, less debonding and longer extension intralaminar fracture than observed in those plies in BF composite. Longer delaminations are observed in the interface between plies -30°/90° and +30°/90°, in comparison to BF composite[25,26].

In Table 1, tensile strength and specific tensile strength of ring specimen BF and GF composites are reported. In Figures 8 and 9, each column is the mean value result (six specimens of each composite) with standard deviations (vertical bars). As presented in Figure 8, BF composite showed 45% higher apparent hoop tensile strength compared to GF composite. Results found in literature comparing these composites strength are between 13-15% higher[12,27,28], and the more pronounced difference can be explained by the higher average wall thickness of BF in comparison to GF composite specimens[29, 30]. Without the effect of difference in wall thickness, another circumferential strength test like hydrostatic test could be used to verify the higher strength of tubular BF composite in comparison to GF composite.

Table 1. Tensile strength and specific tensile strength of ring specimen BF and GF composites.

Specimen	Ultimate tensile strength (MPa)	Ultimate specific tensile strength (MPa. $dm^3.kg^{-1}$)	Specimen	Ultimate tensile strength (MPa)	Ultimate specific tensile strength (MPa. $dm^3.kg^{-1}$)
B1	768	390	V1	499	257
B2	714	360	V2	494	251
B3	711	357	V3	490	253
B4	705	353	V4	498	257
B5	738	380	V5	503	262
B6	727	367	V6	521	265
Mean	727	368	Mean	501	258
Std. dev.	23	14	Std. dev.	11	5

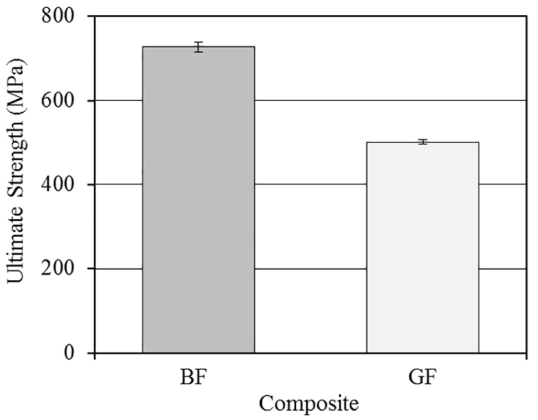

Figure 8. Comparison of ring tensile ultimate strength between BF and GF composites (mean values).

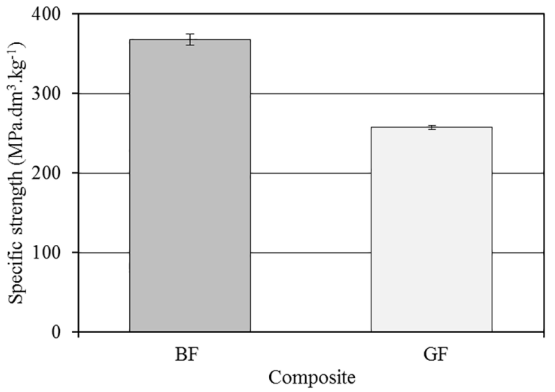

Figure 9. Comparison of ring tensile specific strength between BF and GF composites (mean values).

4. Conclusions

BF composite overcomes GF in the mechanical properties of apparent hoop tensile strength and interlaminar shear stress. BF composite apparent hoop tensile strength is 45% higher than GF composite. The ILSS is 11% higher for BF than GF composite, which indicates better interface adhesion between BF and the epoxy matrix than GF. Less debonding observed in the fracture of BF composite split disk specimens, on 90° angle plies, also represents higher adhesion between BF and the epoxy matrix than GF, in addition to higher ILSS value found for BF composite. Higher difference between apparent tensile strength values of BF and GF composites was found, in comparison to available tensile strength values. New data obtained in this work on mechanical properties of BF composite tubes confirms the literature for BF composite with other geometries, reasserting the applications potential of BF in substitution of GF composites.

5. References

1. Artemenko SE. Polymer Composite Materials Made from Carbon, Basalt and Glass Fibres. Structure and Properties. *Fibre Chemistry.* 2003;35(3):226-229.

2. Fazio P. Basalt fiber: from earth an ancient material for innovative and modern application. *Energia, Ambiente e Innovazione.* 2011;3:89-96.

3. Colombo C, Vergani L, Burman M. Static and fatigue characterisation of new basalt fibre reinforced composites. *Composite Structures.* 2012;94(3):1165-1174.

4. Fiore V, Scalici T, Di Bella G, Valenza A. A review on basalt fibre and its composites. *Composites Part B: Engineering.* 2015;74:74-94.

5. Hao LC, Yu WD. Evaluation of thermal protective performance of basalt fibre nonwoven fabrics. *Journal of Thermal Analysis and Calorimetry.* 2010;100(2):551-555.

6. Liu Q, Shaw MT, Parnas RS, McDonnel AM. Investigation of basalt fibre composite aging behaviour for applications in transportation. *Polymer Composites.* 2006;27(5):475-483.

7. Alexander J, Augustine BSM. Free Vibration and Damping Characteristics of GFRP and BFRP Laminated Composites at Various Boundary Conditions. *Indian Journal of Science and Technology.* 2015;8(12).

8. Parnas RS, Shaw MT, Liu Q. Basalt Fiber reinforced polymer composites. *The New England Transportation Consortium*; 2007.

9. Singha K. A Short Review on Basalt Fiber. *International Journal of Textile Science.* 2012;1(4):19-28.

10. Chikhradze NM, Japaridze LA, Abashidze GS. Properties of Basalt Plastics and of Composites Reinforced by Hybrid Fibers in Operating Conditions. In: Hu N, ed. *Composites and Their Applications.* Rijeka: InTech; 2012.

11. Lopresto V, Leone C, De Iorio I. Mechanical characterization of basalt fibre reinforced plastic. *Composites: Part B: Engineering.* 2011;42:717-723.

12. Carmisciano S, De Rosa IM, Sarasini F, Tamburrano A, Valente M. Basalt woven fiber reinforced vinylester composites: Flexural and electrical properties. *Materials & Design.* 2011;32(1):337-342.

13. Pavlovski D, Mislavsky B, Antonov A. CNG cylinder manufacturers test basalt fibre. *Reinforced Plastics.* 2007;51(4):36-39.

14. Akula VMK, Shubert MK. Analysis of Filament Wound Composite Pressure Vessels Using Cylindrical Elements. In: *Proceedings of the 2013 SAMPE Conference*; 2013 May 6-9; Long Beach, CA, USA. p. 926-940.

15. Martins LAL, Bastian FL, Netto TA. Reviewing some design issues for filament wound composite tubes. *Materials & Design.* 2014;55:242-249.

16. Kaynak C, Salim Erdiller E, Parnas L, Senel F. Use of split-disk tests for the process parameters of filament wound epoxy composite tubes. *Polymer Testing.* 2005;24(5):648-655.

17. Huonnic N, Abdelghani M, Mertiny P, McDonald A. Deposition and characterization of flame-sprayed aluminum on cured glass and basalt fiber-reinforced epoxy tubes. *Surface & Coatings Technology.* 2010;205(3):867-873.

18. Carvalho O. *Influence of the stacking sequence of layers on the mechanical behavior of polymeric composite cylinders.* [Dissertation]. São Paulo: Instituto de Pesquisas Energéticas e Nucleares (IPEN); 2006.

19. ASTM International. *ASTM D2290 - 12 - Standard Test Method for Apparent Hoop Tensile Strength of Plastic or Reinforced Plastic Pipe.* West Conshohocken: ASTM International; 2012.

20. ASTM International. *ASTM D3171 - 15 - Standard Test Methods for Constituent Content of Composite Materials.* West Conshohocken: ASTM International; 2015.

21. Akay M. *Introduction to Polymer Science and Technology.* Mustafa Akay & Ventus Publishing ApS. 2012; 169 p.

22. ASTM International. *ASTM D2344/D2344M - 13 - Standard Test Method for Short-Beam Strength of Polymer Matrix Composite Materials and Their Laminates.* West Conshohocken: ASTM International; 2013.

23. Rajanish M, Nanjundaradhya NV, Sharma RS. Influence of Nano-Modification on the Interlaminar Shear Strength of Unidirectional Glass Fiber-Reinforced Epoxy Resin. *Journal of Minerals and Materials Characterization and Engineering.* 2014;2(4):264-269.

24. Zhou J, Li Y, Li N, Hao X, Liu C. Interfacial shear strength of microwave processed carbon fiber/epoxy composites characterized by an improved fiber-bundle pull-out test. *Composites Science and Technology.* 2016;133:173-183.

25. Greenhalgh ES. *Failure Analysis and Fractography of Polymer Composites.* Boca Raton: CRC Press; 2009. p. 226-227.

26. Hull D. *Fractography: Observing, Measuring, and Interpreting Fracture Surface Topography.* New York: Cambridge University Press; 1999.

27. Lapena MH, Marinucci G, De Carvalho O. Mechanical characterization of unidirectional basalt fiber epoxy composite. In: *Proceedings of the 16th European Conference on Composite Materials ECCM-16*; 2014 Jun 22-26; Seville, Spain.

28. Erdiller ES. *Experimental Investigation for Mechanical Properties of Filament Wound Composite Tubes.* [Thesis]. Ankara: Middle East Technical University; 2004.

29. Pechulis M, Vautour D. The Effect of Thickness on the Tensile and Impact Properties of Reinforced Thermoplastics. *Journal of Reinforced Plastics and Composites.* 1998;17(17):1580-1586.

30. Banakar P, Shivananda HK, Niranjan HB. Influence of Fiber Orientation and Thickness on Tensile Properties of Laminated Polymer Composites. *International Journal of Pure & Applied Sciences and Technology.* 2012;9(1):61-68.